Realistic description of electron-energy-loss spectroscopy for one-dimensional Sr_2CuO_3

A. Hübsch,[1] J. Richter,[1] C. Waidacher,[1] K. W. Becker,[1] and W. von der Linden[2]
[1]*Institut für Theoretische Physik, Technische Universität Dresden, D-01062 Dresden, Germany*
[2]*Institut für Theoretische Physik, Technische Universität Graz, Petersgasse 16, A-8010 Graz, Austria*
(Received 13 November 2000; published 13 April 2001)

We investigate the electron-energy-loss spectrum of one-dimensional undoped CuO_3 chains within an extended multiband Hubbard model and an extended one-band Hubbard model, using the standard Lanczos algorithm. Short-range intersite Coulomb interactions are explicitly included in these models, and long-range interactions are treated in the random-phase approximation. The results for the multiband model with standard parameter values agree very well with experimental spectra of Sr_2CuO_3. In particular, the width of the main structure is correctly reproduced for all values of momentum transfer. We find no evidence for enhanced intersite interactions in Sr_2CuO_3.

DOI: 10.1103/PhysRevB.63.205103 PACS number(s): 71.27.+a, 71.45.Gm, 71.10.Fd

One-dimensional systems are easy to conceive in theory but hard to find in nature, and their experimental realization is restricted to a few materials. These include mesoscopic systems like single-wall nanotubes[1,2] or chains of metal atoms,[3–5] and macroscopic systems with a strong anisotropy in one spatial direction. Among the latter, Sr_2CuO_3 has been the focus of recent research. It contains separated chains of corner-sharing CuO_4 plaquettes, and is related to high-temperature superconducting compounds of higher dimensionality. Generally, the electronic properties of Sr_2CuO_3 are dominated by strong correlations of the valence holes. The low-dimensional character of magnetic excitations in this material manifests itself in magnetic susceptibility measurements that have been successfully described in terms of a one-dimensional spin-$\frac{1}{2}$ Heisenberg antiferromagnet.[6–8]

Charge excitations in Sr_2CuO_3 have recently been investigated[9] by means of electron-energy-loss spectroscopy (EELS). The experimental spectra are shown in the right panel of Fig. 1. In the following we will discuss only the spectral region below 4 eV energy loss. Excitations at higher energies probably involve Sr orbitals, which are not included in models for the Cu-O structure.[9] In the low-energy region the experimental data show a broad dominant low-energy structure at 2.4 eV for momentum transfer $\mathbf{q}=0.1$ Å^{-1}, which shifts to 3.2 eV for $\mathbf{q}=0.8$ Å^{-1} (see Fig. 1). The behavior of this structure as a function of momentum transfer is rather unusual: with increasing momentum transfer up to 0.4 Å^{-1} the width of the structure decreases but increases again for $\mathbf{q}>0.4$ Å^{-1}. These spectra have been interpreted using an extended one-band Hubbard model,[9] an effective two-band Hubbard model,[10] and a multiband Hubbard model.[11] Although the main difference between these models is just the elimination of the oxygen degrees of freedom, the results have been controversial. In the one-band model the behavior of the low-energy feature has been interpreted as the transfer of spectral weight from a continuum of excitations to an exciton, formed due to a strongly enhanced intersite Coulomb repulsion V.[9,12] Excitonic features have also been discussed in the strong coupling limit of an effective two-band Hubbard model.[10] However, the coupling strengths used are not experimentally relevant. Therefore, no direct comparison to experimental data was possible in Ref. 10. In contrast, in the multiband model the dispersion of the low-energy feature has been explained in terms of a shift from a rather delocalized Zhang-Rice singletlike excitation to a more localized one.[11] However, no intersite Coulomb repulsion was included in the Hamiltonian.

Up to now, all theoretical approaches have failed to correctly describe the discussed decrease and increase in spectral width of the low-energy feature as a function of increasing momentum transfer. For small momentum transfer, the

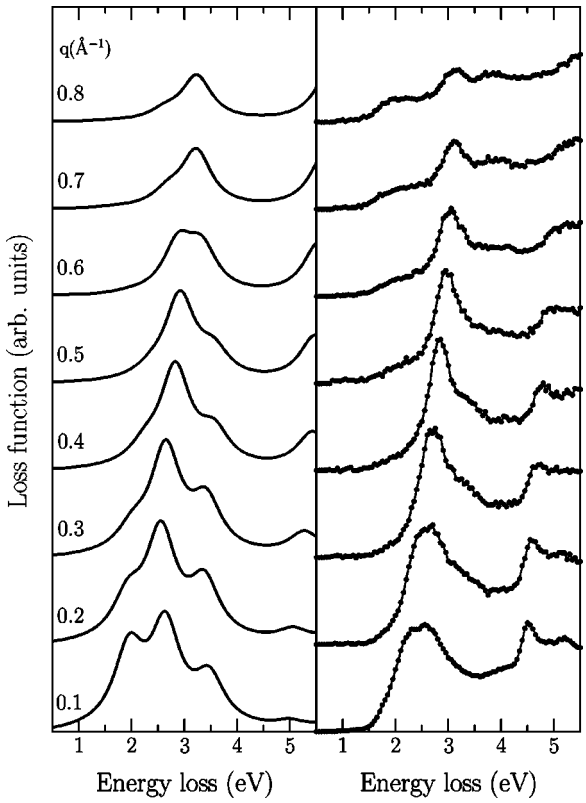

FIG. 1. Comparison of experimental data for Sr_2CuO_3 (right panel), taken from Ref. 9, and the results of the exact diagonalization (left panel). The parameter set is $U_d=8.8$ eV, $\Delta=3.0$ eV, $V_{pd}=1.2$ eV, $V_{dd}=0$ eV, $t_{pd}=1.3$ eV, and $t_{pp}=0.65$ eV. The theoretical line spectra have been convoluted with a Gaussian function of width 0.35 eV.

one-band model overestimates the experimentally observed width by a factor of about 2.[9] In addition, the broadening for large momentum transfer is too small. The analytical approach to the multiband model, on the other hand, underestimates the broadening due to the neglect of far reaching excitations that are important at small momentum transfer.[11]

In this paper, we show that the multiband model provides a realistic description of the EELS spectrum for Sr_2CuO_3, and we observe the correct spectral form for all values of momentum transfer. Furthermore, it is found that the main effect of the intersite Coulomb repulsion is to lead to an energy shift of the EELS spectra. Finally, we discuss the relation of our results to the loss function of the one-band model.

We investigate the dielectric response of a one-dimensional extended multiband Hubbard Hamiltonian at half filling, i.e., a chain of corner-sharing CuO_4 plaquettes with one hole per Cu site. In the hole picture this Hamiltonian reads[13,14]

$$H=\Delta\sum_{j\sigma} n^p_{j\sigma}+U_d\sum_i n^d_{i\uparrow}n^d_{i\downarrow}+V_{pd}\sum_{\langle ij\rangle} n^p_j n^d_i+V_{dd}\sum_{\langle ii'\rangle} n^d_i n^d_{i'}$$
$$+t_{pd}\sum_{\langle ij\rangle\sigma}\phi^{ij}_{pd}(p^\dagger_{j\sigma}d_{i\sigma}+\text{H.c.})+t_{pp}\sum_{\langle jj'\rangle\sigma}\phi^{jj'}_{pp}p^\dagger_{j\sigma}p_{j'\sigma}. \tag{1}$$

The operators $d^\dagger_{i\sigma}$ ($p^\dagger_{j\sigma}$) create a hole with spin σ in the ith Cu $3d$ orbital (jth O $2p$ orbital), and $n^d_{i\sigma}$ ($n^p_{j\sigma}$) are the corresponding number operators, with $n^d_i=n^d_{i\uparrow}+n^d_{i\downarrow}$. The first four terms in Eq. (1) are the atomic part of the Hamiltonian, with the charge-transfer energy Δ, the Cu on-site Coulomb repulsion U_d, the Cu-O intersite repulsion V_{pd}, and the Cu-Cu intersite repulsion V_{dd}. The last two terms in Eq. (1) describe the hybridization of Cu $3d$ and O $2p$ orbitals (hopping strength t_{pd}) and of O $2p$ orbitals (hopping amplitude t_{pp}). ϕ^{ij}_{pd} and $\phi^{jj'}_{pp}$ give the correct sign for the hopping processes, and $\langle ij\rangle$ denotes the summation over nearest neighbor pairs. The Hamiltonian (1) takes account of both in-chain and out-of-chain oxygen sites. Notice that no perturbative approximations are made, so that parameter values can be chosen in the experimentally relevant range.

The dynamical density-density correlation function is directly proportional to the loss function in EELS experiments.[15] By including the long-range Coulomb interaction in the model within a random-phase approximation[16] one finds for the loss function

$$L(\omega,\mathbf{q})=\text{Im}\left[\frac{-1}{1+v_{\mathbf{q}}\chi^0_\rho(\omega,\mathbf{q})}\right], \tag{2}$$

where

$$\chi^0_\rho(\omega,\mathbf{q})=\frac{i}{\hbar}\int_0^\infty dt\, e^{i\omega t}\langle 0|[\rho_{\mathbf{q}}(t),\rho_{-\mathbf{q}}]|0\rangle \tag{3}$$

is the response function at zero temperature of the short-range interaction model (1). χ^0_ρ depends on the energy loss ω and momentum transfer $\mathbf{q}$. $|0\rangle$ is the ground state, $\rho_{\mathbf{q}}$ denotes the Fourier transform of n_i, and $v_{\mathbf{q}}=e^2N/(\epsilon_0\epsilon_r v\mathbf{q}^2)$ is the long-range Coulomb interaction with unit cell volume v. N is the number of electrons per unit cell, and ϵ_0 is the permittivity. The real part ϵ_r of the dielectric function can be obtained from the experiment. In the case of Sr_2CuO_3 it was found to be $\epsilon_r=8$.[9] In the following we evaluate Eq. (2) using the standard Lanczos algorithm[17] which is limited to small clusters. The theoretical line spectra are convoluted with a Gaussian function of width 0.35 eV, to allow a comparison with experiment.

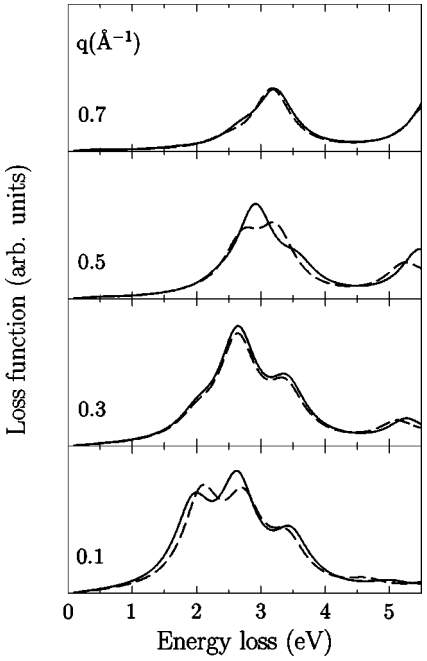

FIG. 2. Finite-size effects in the loss function of model (1) for clusters with six plaquettes (full lines) and five plaquettes (dashed line), with open boundary conditions. Parameters as for Fig. 1.

First we check if our results are sufficiently converged with respect to system size. In Fig. 2 we compare the loss function of clusters with five (dashed lines) and six plaquettes (full lines). In both cases open boundary conditions are chosen. One has to make sure that holes on the edges of the cluster are still embedded in the local Coulomb potential that results from a state with occupied Cu sites. For this purpose, O (Cu) sites on the edge of the cluster are assigned an additional on-site energy due to V_{pd} (V_{dd}). As can be seen from Fig. 2, there are only small finite-size effects. Thus we conclude that the cluster with six plaquettes is large enough to obtain reliable results.

In Fig. 1 the calculated loss function is compared to the experimental spectra from Ref. 9. The parameters in the model Hamiltonian are chosen as follows. $U_d=8.8$ eV, $V_{pd}=1.2$ eV, $V_{dd}=0$ eV, $t_{pd}=1.3$ eV, and $t_{pp}=0.65$ eV are kept constant at typical values.[18–20] The value of $\Delta=3.0$ eV has been adjusted to obtain correct peak positions. This means that we use only one free parameter. As compared to the standard value 3.5 eV for Δ,[18–20] the smaller Δ is in agreement with theoretical analysis of x-ray photoemission spectra for Sr_2CuO_3.[21–23,25] Notice that a small value of Δ

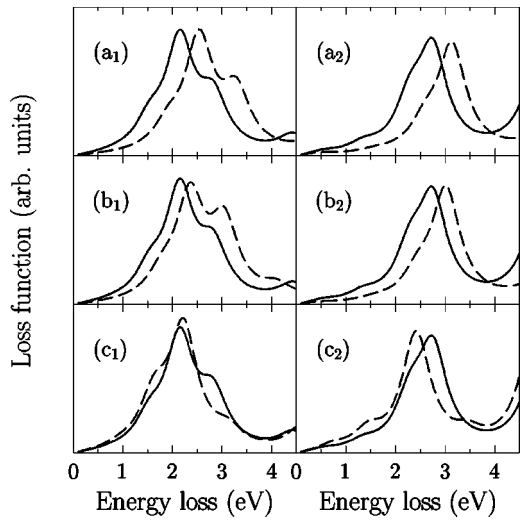

FIG. 3. Influence of V_{pd}, Δ, and V_{dd} on the loss functions with momentum transfer $\mathbf{q}=0.3$ Å^{-1} (left side) and $\mathbf{q}=0.7$ Å^{-1} (right side); other parameters as for Fig. 1. In (a) $\Delta=3.0$ eV and V_{dd} are kept constant and V_{pd} is varied (full lines, $V_{pd}=0$; dashed lines, $V_{pd}=1.0$ eV); in (b) Δ is varied (full lines, $\Delta=3.0$ eV; dashed lines, $\Delta=4.0$ eV) for $V_{pd}=V_{dd}=0$; and in (c) $\Delta=3.0$ eV and $V_{pd}=0$ are constant (full lines, $V_{dd}=0$; dashed lines, $V_{dd}=0.5$ eV). The loss functions with $\mathbf{q}=0.3$ Å^{-1} and $\mathbf{q}=0.7$ Å^{-1} are scaled independently of each other.

means that the system is not in the strong coupling limit as was assumed in Ref. 10. The calculated loss function consists of a dominant structure at 2.5 eV for $\mathbf{q}=0.1$ Å^{-1}, which shifts to 3.2 eV for $\mathbf{q}=0.8$ Å^{-1}. In addition, a second excitation is observed at 5.5 eV. In agreement with the experimental observation, with increasing momentum transfer the main structure shifts to higher energies and first decreases in width. For $\mathbf{q}>0.4$ Å^{-1} the spectral width increases again. The main structure results from excitations in which a hole leaves its original plaquette to form Zhang-Rice singletlike states[24] with neighboring holes. With increasing momentum transfer $\mathbf{q}$ the spectral weight shifts from extended to more localized excitations.[11]

Next we discuss the dependence of the calculated spectra on the different parameters in Hamiltonian (1). In agreement with an analysis[25] of the optical conductivity for Sr_2CuO_3 it is found that the main influence of Δ and the intersite Coulomb repulsion V_{pd} is a shift of the excitation energy of the main structure. This is shown in Fig. 3 for V_{pd} [see panels (a_1) and (a_2)] and Δ [see panels (b_1) and (b_2)]. Note that we observe nearly the same results for $\Delta=3.0$ eV, $V_{pd}=1.0$ eV [dashed lines in panels (a_1) and (a_2) of Fig. 3] and $\Delta=4.0$ eV, $V_{pd}=0$ [dashed lines in panels (b_1) and (b_2) of Fig. 3]. Hence, only the sum of both parameters $\Delta+V_{pd}$ is relevant for the spectra. Therefore, it is possible to obtain good agreement between experimental and theoretical spectra with or without intersite Coulomb interaction V_{pd}. This implies that the mechanism of excitations is not driven by a strong intersite interaction V_{pd}. Furthermore, this observation also explains why a fit of a multiband model with $V_{pd}=0$ to the experimental data led to a larger value of Δ in Ref. 11.

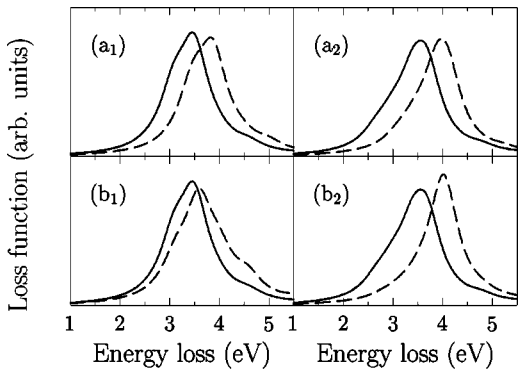

FIG. 4. Influence of the Coulomb interactions U and V of the extended one-band Hubbard model on the loss function with momentum transfer $\mathbf{q}=0.3$ Å^{-1} (left side) and $\mathbf{q}=0.7$ Å^{-1} (right side); parameter values are chosen according to Ref. 9. The hopping strength is $t=0.55$ eV. In (a) $V=1.3$ eV is kept constant (full lines, $U=4.2$ eV; dashed lines, $U=4.7$ eV), and in (b) V is varied (full lines, $V=1.3$ eV; dashed lines, $V=0.8$ eV) for $U=4.2$ eV. The theoretical line spectra have been convoluted with a Gaussian function of width 0.35 eV. The loss functions with $\mathbf{q}=0.3$ Å^{-1} and $\mathbf{q}=0.7$ Å^{-1} are scaled independently of each other.

In contrast to Δ and V_{pd}, the Cu-Cu intersite repulsion V_{dd} does not shift the complete EELS spectra but rather transfers spectral weight to excitations with smaller energy loss [see panels (c_1) and (c_2) of Fig. 3]. A comparison of panels (c_1) and (c_2) shows that this effect is larger near the zone boundary at $\mathbf{q}=0.8$ Å^{-1}. This behavior can probably be connected with formation of an exciton state as discussed in Refs. 9 and 10. On the other hand, the choice $V_{dd}=0$ is a good approximation[26] for the multiband model (1) since the distance between neighboring Cu sites is relatively large. Therefore, possible exciton formation seems not to be relevant for interpretation of the experimental spectra if one uses the multiband model.

Finally, we want to discuss the relation of our results for the multiband model to the loss function (2) of the one-dimensional extended Hubbard model

$$H=-t\sum_{\langle ij\rangle\sigma}(d^{\dagger}_{i\sigma}d_{j\sigma}+\text{H.c.})+U\sum_{i}n^{d}_{i\uparrow}n^{d}_{i\downarrow}+V\sum_{\langle ij\rangle}n^{d}_{i}n^{d}_{j}, \tag{4}$$

which considers only effective Cu $3d$ orbitals. In Eq. (4), t is the hopping strength, U denotes the on-site Coulomb repulsion, and V is the intersite interaction. Note that the mapping of the multiband model (1) onto the one-band model (4) is problematic for the model parameters used above because the system is not in the strong coupling limit. Therefore, we may compare the loss function of both models only qualitatively. In the following, we compute the loss function (2) of the one-band model (4) using a cluster with 12 sites and periodic boundary conditions. If one reduces the multiband model (1) to a one-band model the charge-transfer gap Δ is replaced by the Hubbard gap U of the effective model.[27] Therefore, in analogy to the influence of Δ in the multiband model, increasing U shifts the spectra to higher energy loss [see panels (a_1) and (a_2) of Fig. 4]. In panels (b_1) and (b_2)

of Fig. 4 the loss functions with $\mathbf{q}=0.3$ Å^{-1} and $\mathbf{q}=0.7$ Å^{-1} are shown for $V=1.3$ eV (full lines) and $V=0.8$ eV (dashed lines) where $U=4.2$ eV and $t=0.55$ eV are kept constant at the values from Ref. 9. In analogy to the influence of the intersite Coulomb repulsion V_{dd} in the multiband model discussed above, a moderate increase in V leads mainly to a transfer of spectral weight to excitations with smaller energy loss. However, a nonzero intersite Coulomb repulsion V is needed to obtain spectra related to experiment. This fact led to the conclusion that the spectral intensity at the zone boundary is due to exciton formation.[9] On the other hand, the large differences between the interpretations of the experimental spectra for Sr_2CuO_3 using the one-band[9] and the multiband model imply that oxygen degrees of freedom are important for a realistic description of charge excitations in the cuprates.

In conclusion, we have carried out an investigation of the EELS spectrum for the one-dimensional CuO_3 chain using an extended multiband Hubbard model and an extended Hubbard model. Our results for the multiband model show very good agreement with experimental data for Sr_2CuO_3. In contrast to former investigations, we can explain the width of the main structure for all values of momentum transfer. For the multiband model, only a combination of intersite Coulomb interaction and charge-transfer energy is relevant for the loss function. Consequently, we find no evidence for enhanced intersite interactions in Sr_2CuO_3. The different explanations for the spectral intensity at the zone boundary using the one-band and the more realistic multiband models shows that the oxygen degrees of freedom are important for the description of charge excitations.

We would like to acknowledge fruitful discussions with S. Atzkern, S.-L. Drechsler, J. Fink, M. S. Golden, R. E. Hetzel, R. Neudert, and H. Rosner. This work was supported by DFG through the research programs GK 85 and SFB 463. The calculations were performed on the Origin 2000 at Technische Universität Dresden.

[1] S. Ijima, Nature (London) **345**, 56 (1991).
[2] M. Bockrath, D.H. Cobden, J. Lu, A.G. Rinzler, R.E. Smalley, L. Balents, and P.L. McEuen, Nature (London) **397**, 598 (1999).
[3] H. Brune, M. Giovannini, K. Bromann, and K. Kern, Nature (London) **394**, 451 (1998).
[4] A.I. Yanson, G. Rubio Bollinger, H.E. van den Brom, N. Agrat, and M. van Ruitenbeek, Nature (London) **395**, 783 (1998).
[5] P. Segovia, D. Purdie, M. Hengsberger, and Y. Baer, Nature (London) **402**, 504 (1999).
[6] T. Ami, M.K. Crawford, R.L. Harlow, Z.R. Wang, D.C. Johnston, Q. Huang, and R.W. Erwin, Phys. Rev. B **51**, 5994 (1995).
[7] N. Motoyama, H. Eisaki, and S. Uchida, Phys. Rev. Lett. **76**, 3212 (1996).
[8] K.M. Kojima, Y. Fudamoto, M. Larkin, G.M. Luke, J. Merrin, B. Nachumi, Y.J. Uemura, N. Motoyama, H. Eisaki, S. Uchida, K. Yamada, Y. Endoh, S. Hosoya, B.J. Sternlieb, and G. Shirane, Phys. Rev. Lett. **78**, 1787 (1997).
[9] R. Neudert, M. Knupfer, M.S. Golden, J. Fink, W. Stephan, K. Penc, N. Motoyama, H. Eisaki, and S. Uchida, Phys. Rev. Lett. **81**, 657 (1998).
[10] K. Penc and W. Stephan, Phys. Rev. B **62**, 12 707 (2000).
[11] J. Richter, C. Waidacher, and K.W. Becker, Phys. Rev. B **61**, 9871 (2000).
[12] W. Stephan and K. Penc, Phys. Rev. B **54**, R17 269 (1996).
[13] V.J. Emery, Phys. Rev. Lett. **58**, 2794 (1987).
[14] V.J. Emery and G. Reiter, Phys. Rev. B **38**, 4547 (1988).
[15] S.E. Schnatterly, Solid State Phys. **34**, 275 (1977).
[16] D. Pines and D. Bohm, Phys. Rev. **85**, 338 (1952).
[17] For example, see H.Q. Lin and J.E. Gubernatis, Comput. Phys. **7**, 400 (1993), and references therein.
[18] A.K. Mahan, R.M. Martin, and S. Satpathy, Phys. Rev. B **38**, 6650 (1988).
[19] M.S. Hybertsen, M. Schlüter, and N.E. Christiansen, Phys. Rev. B **39**, 9028 (1989).
[20] J.B. Grant and A.K. McMahan, Phys. Rev. B **46**, 8440 (1992).
[21] K. Okada, A. Kotani, K. Maiti, and D.D. Sarma, J. Phys. Soc. Jpn. **65**, 1844 (1996).
[22] C. Waidacher, J. Richter, and K.W. Becker, Europhys. Lett. **47**, 77 (1999).
[23] C. Waidacher, J. Richter, and K.W. Becker, Phys. Rev. B **61**, 13 473 (2000).
[24] F.C. Zhang and T.M. Rice, Phys. Rev. B **37**, 3759 (1988).
[25] K. Okada and A. Kotani, J. Phys. Soc. Jpn. **66**, 341 (1997).
[26] E. Dagotto, Rev. Mod. Phys. **66**, 763 (1994).
[27] J. Zaanen, G.A. Sawatzky, and J.W. Allen, Phys. Rev. Lett. **55**, 418 (1985).